Accepted Manuscript

Potential of dissimilatory nitrate reduction pathways in polycyclic aromatic hydrocarbon degradation

Hugo Ribeiro, Trelita de Sousa, João P. Santos, António G.G. Sousa, Catarina Teixeira, Maria R. Monteiro, Paula Salgado, Ana P. Mucha, C. Marisa R. Almeida, Luís Torgo, Catarina Magalhães

PII: S0045-6535(18)30188-7

DOI: 10.1016/j.chemosphere.2018.01.171

Reference: CHEM 20752

To appear in: *ECSN*

Received Date: 11 September 2017

Revised Date: 29 January 2018

Accepted Date: 31 January 2018

Please cite this article as: Ribeiro, H., de Sousa, T., Santos, Joã.P., Sousa, Antó.G.G., Teixeira, C., Monteiro, M.R., Salgado, P., Mucha, A.P., Almeida, C.M.R., Torgo, Luí., Magalhães, C., Potential of dissimilatory nitrate reduction pathways in polycyclic aromatic hydrocarbon degradation, *Chemosphere* (2018), doi: 10.1016/j.chemosphere.2018.01.171.

This is a PDF file of an unedited manuscript that has been accepted for publication. As a service to our customers we are providing this early version of the manuscript. The manuscript will undergo copyediting, typesetting, and review of the resulting proof before it is published in its final form. Please note that during the production process errors may be discovered which could affect the content, and all legal disclaimers that apply to the journal pertain.

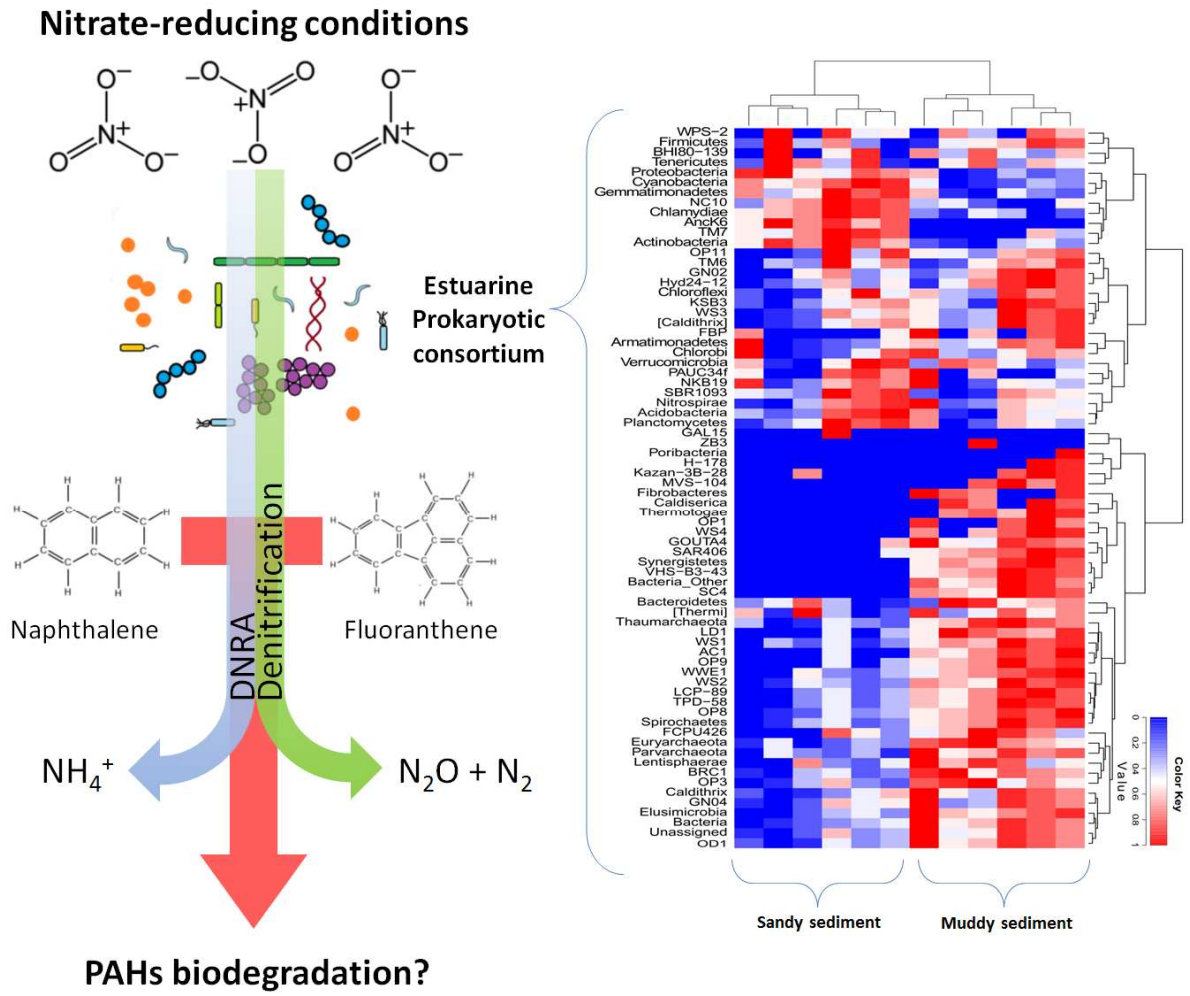
Nitrate-reducing conditions
Estuarine Prokaryotic consortium
Naphthalene
Fluoranthene
DNRA
Denitrification
NH_4^+
$N_2O + N_2$
PAHs biodegradation?
WPS−2
Firmicutes
BHI80−139
Tenericutes
Proteobacteria
Cyanobacteria
Gemmatimonadetes
NC10
Chlamydiae
AncK6
TM7
Actinobacteria
OP11
TM6
GN02
Hyd24−12
Chloroflexi
KSB3
WS3
[Caldithrix]
FBP
Armatimonadetes
Chlorobi
Verrucomicrobia
PAUC34f
NKB19
SBR1093
Nitrospirae
Acidobacteria
Planctomycetes
GAL15
ZB3
Poribacteria
H−178
Kazan−3B−28
MVS−104
Fibrobacteres
Caldiserica
Thermotogae
OP1
WS4
GOUTA4
SAR406
Synergistetes
VHS−B3−43
Bacteria_Other
SC4
Bacteroidetes
[Thermi]
Thaumarchaeota
LD1
WS1
AC1
OP9
WWE1
WS2
LCP−89
TPD−58
OP8
Spirochaetes
FCPU426
Euryarchaeota
Parvarchaeota
Lentisphaerae
BRC1
OP3
Caldithrix
GN04
Elusimicrobia
Bacteria
Unassigned
OD1
Color Key
Value
0
0.2
0.4
0.6
0.8
1
Sandy sediment
Muddy sediment

ACCEPTED

ACCEPTED MANUSCRIPT

Potential of dissimilatory nitrate reduction pathways in polycyclic aromatic hydrocarbon degradation

Running title: Potential nitrate reducing pathways in PAH degradation

Hugo Ribeiro[1 § *], Trelita de Sousa[1,2 §], João P. Santos[1], António G. G. Sousa[1,4], Catarina Teixeira[1,3], Maria R. Monteiro[1], Paula Salgado[1,3], Ana P. Mucha[1], C. Marisa R. Almeida[1], Luís Torgo[4,5], Catarina Magalhães[1,4 §]

[1] CIMAR/CIIMAR-Centro Interdisciplinar de Investigação Marinha e Ambiental, Universidade do Porto, Terminal de Cruzeiros do Porto de Leixões, Av. General Norton de Matos s/n, 4450-208 Matosinhos, Portugal

[2] Department of Microbiology, Goa University, Taleigao Plateau, Goa – 403206

[3] ICBAS - Instituto de Ciências Biomédicas de Abel Salazar (ICBAS-UP), Universidade do Porto, Porto, Portugal

[4] FCUP – Faculdade de Ciências da Universidade do Porto, Porto, Portugal

[5] INESC TEC – INESC Technology and Science, Porto Portugal

[§] These authors contributed equally to this work

***Corresponding author**

Phone (+351) 22 340 18 54

Email: hribeiro@ciimar.up.pt

Abstract

This study investigates the potential of an indigenous estuarine microbial consortium to degrade two polycyclic aromatic hydrocarbons (PAHs), naphthalene and fluoranthene, under nitrate-reducing conditions. Two physicochemically diverse sediment samples from the Lima Estuary (Portugal) were spiked individually with 25 mg L^{-1} of each PAH in laboratory designed microcosms. Sediments without PAHs and autoclaved sediments spiked with PAHs were run in parallel. Destructive sampling at the beginning and after 3, 6, 12, 30 and 63 weeks incubation was performed. Naphthalene and fluoranthene levels decreased over time with distinct degradation dynamics varying with sediment type. Next-generation sequencing (NGS) of 16S rRNA gene amplicons revealed that the sediment type and incubation time were the main drivers influencing the microbial community structure rather than the impact of PAH amendments. Predicted microbial functional analyses revealed clear shifts and interrelationships between genes involved in anaerobic and aerobic degradation of PAHs and in the dissimilatory nitrate-reducing pathways (denitrification and dissimilatory nitrate reduction to ammonium - DNRA). These findings reinforced by clear biogeochemical denitrification signals (NO_3^- consumption, and NH_4^+ increased during the incubation period), suggest that naphthalene and fluoranthene degradation may be coupled with denitrification and DNRA metabolism. The results of this study contribute to the understanding of the dissimilatory nitrate-reducing pathways and help uncover their involvement in degradation of PAHs, which will be crucial for directing remediation strategies of PAH-contaminated anoxic sediments.

Keywords: Naphthalene; fluoranthene; polycyclic aromatic hydrocarbons; denitrification; dissimilatory nitrate reduction to ammonium

ACCEPTED MANUSCRIPT

1. Introduction

Polycyclic aromatic hydrocarbons (PAHs) are formed during incomplete combustion or pyrolysis of organic compounds like those found in coal, oil and wood (Rengarajan et al. 2015). The US Environmental Protection Agency (US EPA) has identified 16 PAHs of most concern (including naphthalene and fluoranthene) based on their ecotoxicity and potential carcinogenicity. The high hydrophobicity, chemical stability, low volatility and high affinity for sediment particles of these PAHs enable them to persist in the environment (Chauhan et al. 2008). Therefore, understanding their behavior in the environment is particularly important. Natural microbial populations play a dominant role during the degradation process, and bioremediation using indigenous microbial communities is recognized as the best strategy to remove these hazardous compounds (Jain et al. 2011). Diverse groups of microorganisms can use petroleum hydrocarbons as the sole carbon and energy source (reviewed by Head et al. 2006; Joye et al. 2016). Two- and three-ring PAHs can be degraded anaerobically, but PAHs with more than three rings are among the most difficult compounds to degrade biologically (reviewed by Meckenstock et al. 2016; Rabus et al. 2016). PAHs are known to affect bacterial community composition and activity (reviewed by Rabus et al. 2016), however, little is known about the relationship between the microbial community shifts and the actual PAHs degradation.

Due to the dynamic effect of weathering and tidal action on oil spills, the partially water-soluble aromatic hydrocarbons including PAHs are ultimately deposited in anoxic ecosystems such as deep sediments and deep sea aquifers (Cao et al. 2009; De Sousa 2015). Several studies have revealed that anaerobic pathways are responsible for most sub-surface hydrocarbon degradation in petroleum reservoirs mostly coupled with microbial processes like denitrification, iron (III) reduction, sulphate reduction and methanogenesis (Cao et al. 2009; Rabus et al. 2016). In terms of energy acquisition and anaerobic degradation rates, NO_3^- is the preferred electron acceptor in comparison to Fe^{3+}, SO_4^{2-} and CO_2 (Ladino-Orjuela et al. 2015). In fact, NO_3^- increases the efficiency of hydrocarbon biodegradation in comparison to SO_4^{2-}, chlorate and Fe^{3+} (Van der Zaan et al. 2012). Amendment with N (in different forms) is usually used to stimulate the catabolic capacity of microbial communities involved in oil bioremediation (Varjani and Upasani 2017). Nitrate is an electron acceptor for cellular metabolism rather than for cell synthesis in both denitrification and dissimilatory nitrate reduction to ammonium (DNRA) pathways (Tiedje 1988). Denitrification represents a permanent nitrogen removal pathway by reducing NO_3^- to dinitrogen gas (N_2) (Knowles 1982; Zumft 1997); while DNRA is a nitrogen-conserving mechanism that transforms NO_3^- to another more bio-available inorganic-N form, ammonium (NH_4^+) (Tiedje 1988).

Nitrate reducing populations are prevalent in petroleum contaminated systems (Joye et al. 2014), making them model candidates for oil-related bioremediation designs. Although several studies suggested anaerobic degradation of PAHs with nitrate as the electron acceptor (reviewed by Rabus et al. 2016), there is still a lack of knowledge about the metabolism of aromatic hydrocarbon degradation under nitrate reducing conditions, including the pathways and microbial communities involved and the significance of those metabolic pathways in natural ecosystems. The current known anaerobic pathways that could be involved in the first activation step of aromatic hydrocarbons are the direct carboxylation, anaerobic hydroxylation, fumarate addition, and methylation followed by fumarate addition (reviewed by Ladino-Orjuela et al. 2015; Ghattas et al. 2017). Recently, Meckenstock *et al.* (2016) noted the difficulty to reproduce PAHs degradation by nitrate-reducing cultures with nitrate as the electron acceptor. Moreover, it has been reported that under anoxic conditions, a methane-oxidizing denitrifying bacterium (*Candidatus* Methylomirabilis oxyfera) and the alkane-oxidizing ϒ-proteobacterium (HdN1) might produce oxygen through disproportionation of the nitric oxide (NO) (Ettwig et al. 2010; Zedelius et al. 2011; Zhu et al. 2017). In fact, according to Zhu *et al.* (2017), the genes (*nod*) putatively involved in the disproportionation of NO to oxygen have wide-spread occurrence and diversity in the aromatic hydrocarbons contaminated aquifers and nitrogen removing wastewater treatment systems. Although the underlying oxygen generation mechanism is still elusive, the initial or/and complete PAHs degradation could be due to aerobic pathways, particularly under microaerophilic conditions.

The present study hypothesizes that microbial consortia indigenous to estuarine systems can degrade naphthalene and fluoranthene under nitrate-reducing conditions. Furthermore, we suggest that nitrate reducing conditions would foster denitrifiers and DNRA bacteria, therefore the study also aimed at evaluating the shifts induced by PAHs in the prokaryotic communities. Lastly, this study is an attempt to evaluate the potential of anaerobic biodegradation of naphthalene and fluoranthene in estuarine sediments with distinct characteristics.

2. Materials and Methods

2.1. Study area

The NW Atlantic Coast of Portugal is in the vicinity of a major oil tanker route and therefore chronically exposed to petroleum hydrocarbon contamination (Ribeiro et al. 2013a). After the Prestige oil spill of 2002 and various other navigation accidents of smaller magnitude, several studies have reported the presence of PAHs in the Lima and Douro estuaries and their harmful consequences to the marine ecosystems of the Iberian Atlantic Coast (Ribeiro et al. 2013a).

The Lima River Estuary (41.41 °N; 8.48 °W) is a highly industrialized estuary and prone to excessive anthropogenic navigation, shipping and fishing activities in the lower estuary. Moreover, this area is exposed to petroleum contamination due to its proximity to important maritime traffic routes, an oil refining industry and two maritime harbors located at Leixões and Viana do Castelo.

Sediment samples were collected in October 2014 from two sites along the Lima Estuary, one relatively undisturbed site (L1) and one anthropogenically influenced site (L3), selected based on available literature and previous field surveys (Ribeiro et al. 2013b; Ribeiro et al. 2015; Ribeiro et al. 2016). Site L1 is located upstream of River Lima while L3 site lies downstream of the river, very close to the seaport and dredging zone and more vulnerable to the pollutants emerging from the shipyard, fishing harbor and marina activities nearby.

2.2. Sampling and sediment characterization

Sediments were collected from a depth of 5 cm during low tide, homogenized in sterile plastic bags and transported in the dark to the laboratory for processing in refrigerated ice chests. Collected sediments were characterized in terms of sand characteristics, denitrification potential, PAH levels and total viable counts (TVCs) by the methods described below. Total organic matter (OM) content was measured as a percentage of weight loss by incineration (500 °C, 4 h), and grain size distribution by dry sieving (Ribeiro et al. 2011).

2.3. Determination of Total Viable Counts of nitrate reducing bacteria

Total viable counts (TVC) of nitrate reducing bacteria in L1 and L3 triplicate samples were determined using appropriate dilutions of the samples in sterile saline water (0.85 % NaCl in distilled water) were plated on nitrate reduction medium (NRM, nutrient broth supplemented with 0.1 % KNO_3 and 2 % agar) (Atlas and Parks 1997) and modified bromothymol blue (BTB) medium (Takaya et al. 2003) containing (per liter) 8.5 g sodium succinate, 1 g KNO_3, 1 g KH_2PO_4, 1 g $MgSO_4.7H_2O$, 0.5 g $FeSO_4.7H_2O$, 0.2 g $CaCl_2.7H_2O$, 1 mL bromothymol blue solution (10 mg bromothymol blue powder dissolved in 1 mL absolute ethanol), 20 g agar and pH adjusted to 7.2. NRM is a nutrient rich medium that works like nutrient agar but also enriches nitrate reducing bacteria including denitrifiers, bacteria involved in DNRA and nitrate assimilating bacteria (Atlas and Parks 1997). On the other hand, BTB medium is specially designed to enrich the isolation of cultivable denitrifying and DNRA bacteria which display blue halos around their colonies due to depletion of nitrate and subsequently nitrite from the medium (Takaya et al. 2003; Wang et al. 2007a). Bacterial colonies were counted and TVC calculated as colony forming units (CFU) mL^{-1} of the sample.

168 **2.4. Degradation of PAHs under nitrate reducing conditions in laboratory designed**
169 **microcosms**

170 Laboratory controlled microcosms were designed to study the anaerobic degradation of
171 naphthalene and fluoranthene, under nitrate-reducing conditions. Twenty mL (18 ± 0.5 g) of
172 sediment from L1 and L3, respectively, were placed in sterile triplicate 50 mL serum bottles. The
173 bottles were then filled with 20 mL of sterile Difco Bushnell-Haas (BH), as liquid medium, containing
174 (per liter) 1 g KNO_3, 1 g KH_2PO_4, 0.2 g $MgSO_4.7H_2O$, 0.05 g $FeCl_3$, 0.02 g $CaCl_2.7H_2O$, 1 g $(NH_4)_2HPO_4$
175 and amended with 1 % NaCl and pH adjusted to 7 ± 0.2. The serum bottles were hermetically sealed
176 with sterile Teflon-lined butyl septa and aluminum crimps, purged with N_2 gas to remove the oxygen
177 and maintain anoxic conditions. Naphthalene and fluoranthene were added individually to the
178 medium at a final concentration of 25 mg L^{-1} (1000 µg of each PAH dissolved in dichloromethane).
179 Sediment controls (without PAH) were setup to assess naphthalene and fluoranthene effect on
180 microbial communities and activities. Triplicate sterile controls (autoclaved five times during 30 min
181 at 121 °C) were setup to assess abiotic losses of naphthalene and fluoranthene after the 63 weeks of
182 incubation. The bottles were incubated in the dark at 20 °C under static conditions for 63 weeks.
183 Destructive sampling of the serum bottles (in triplicate for each treatment) was performed at the
184 beginning of the experiment and at time intervals of 3, 6, 12, 30 and 63 weeks of incubation. The
185 following analyses were performed at referred intervals. At week 33 and 60, autoclaved potassium
186 nitrate (KNO_3) was added to all L3 sediments serum bottles (control, and to sediments spiked with
187 naphthalene and fluoranthene) to replenish NO_3^- consumed. In L1 sediment serum bottles there was
188 no significant depletion of nitrate warranted amendment.
189

190 **2.5. PAH measurements by GC-MS**

191 The PAH levels were determined in both liquid medium and sediments by gas chromatography (GC)
192 following previously optimized and validated procedures (Gonçalves et al. 2016). Briefly, two
193 replicates of 0.25 g of lyophilized sediment samples were extracted with 5 mL HPLC Grade methanol,
194 sonicated (Elma Transsonic 460H) for 30 min and centrifuged at 3000 rpm for 5 min. Then, the
195 extract was shaken during 10 min with 300 mg of florisil, followed by an additional centrifugation
196 step. Fifty µL of the methanolic extract were added to a 20-mL amber vial and diluted with water to
197 a final volume of 10 mL. Liquid medium was analyzed without further treatment, a total volume of
198 10 mL being also analyzed in similar 20-mL amber vials. Prior to GC analysis, an internal standard (IS)
199 solution (EPA 8270 Semi-volatile Internal Standard mix, Supelco) containing five deuterated PAHs
200 was added to all solutions (both liquid medium and diluted sediment extract) in the 20-mL amber
201 vials. These solutions were subject to Headspace Solid Phase Micro Extraction (HS-SPME) employing

202 a 100 µm polydimethylsiloxane (PDMS) fiber. The SPME fiber was introduced in the headspace of the
203 20-mL amber vial, which was tightly capped with Teflon-lined septa, and extraction was performed,
204 with agitation at 250 rpm, at 60 °C during 60 min. The fiber was then transferred to the GC injection
205 port for desorption during 15 min (5 min in splitless mode) at 280 °C. Chromatographic analyses
206 were carried out in a Varian 3900 mounted with a Zebron ZB-5MS capillary column (60 m x 0.25 mm
207 i.d. x 0.25 µm film thickness). The carrier gas was helium of high purity flowing at 1 mL min^{-1}. The GC
208 oven temperature program was established as follows: initial temperature 40 °C (held 1 min),
209 ramped at 40 °C min^{-1} to 150 °C, ramped at 3.4 °C min^{-1} to 280 °C (held 1 min) and, finally, increased
210 by 4 °C min^{-1} to 300 °C and held at this temperature for 14.01 min. The GC was coupled with a Varian
211 Saturn 2000 ion trap mass spectrometer operated in the EI mode. Selected ion storage (SIS) mode
212 was used for quantitation (Gonçalves et al. 2016). For PAHs quantification, PAHs standard solutions
213 prepared from a stock solution of 16 EPA priority PAHs (Fluka) were analyzed as samples and
214 calibration curves calculated using the ratio of PAHs standard solutions signals to the deuterated IS.
215 More details can be found in Gonçalves et al. (2016).
216

217 **2.6. Nutrient analyses**

218 At zero time and at the time intervals of 3, 6, 12, 30 and 63 weeks, 2 mL of medium sample were
219 taken from each serum bottle in triplicates, centrifuged at 8000 rpm for 10 min and stored at -20 °C
220 for later nutrient (nitrate, nitrite and ammonia) quantification (Magalhães et al. 2005). The
221 ammonium (NH_4^+) and nitrite (NO_2^-) concentrations were quantified as described by Grasshoff et al.
222 (1983), and nitrate (NO_3^-) plus NO_2^- determined using the spongy cadmium reduction technique
223 (Jones 1984). The actual NO_3^- concentration was calculated as the difference between NO_3^- + NO_2^-
224 and NO_2^-. The detection limit was 0.1, 0.02 and 0.3 µM respectively for NH_4^+, NO_2^-, NO_3^- and the
225 precision of all determinations was between 0.1 and 8 %, depending on the particular nutrient
226 concentration.
227

228 **2.7. Denitrification and N_2O production rates**

229 The acetylene method was used to measure denitrification rates in all sediments incubated as anoxic
230 slurries in the laboratory designed microcosms. Denitrification and nitrous oxide (N_2O) potential
231 rates were measured at zero time and at regular intervals (3, 6 and 12, 30 and 63 weeks) according
232 to Magalhães et al. (2005). The bottles were analyzed in triplicate with and without acetylene (20 %
233 v/v) and incubated in the dark for 4 h with constant stirring at 70 rpm. At the end of the incubation
234 period, 12 mL of gas was collected from the headspace of each serum bottle and stored in a 12 mL
235 serum vial, which was previously degassed. The gas collection was carried out with simultaneous

236 displacement with 12 mL of 3 M NaCl solution. N_2O was quantified in a Bruker gas chromatograph
237 (430-GC) equipped with an electron capture detector (ECD) with two Hay Sep D columns at 100 °C
238 and an automatic backflush system to prevent C_2H_2 from passing to the detector (Magalhães et al.
239 2005). A mixture of 5 % methane in argon was used as the carrier gas. The retention time of N_2O was
240 1.6 min and its concentration was calculated using a standard curve generated from certified gas
241 standards (N_2O in He). The detection limit for N_2O was 15 nM. Denitrification (N_2 production) was
242 calculated as the difference between the N_2O produced with and without acetylene (Magalhães et
243 al. 2005).
244

245 **2.8. 16S rDNA amplicon sequencing and analysis**

246 Composite samples from L1 and L3 sediment after 12 and 63 weeks of incubation were selected for
247 sequencing. Sequencing process including amplification of 16S rRNA gene fragment (V4-V5
248 hypervariable regions) was carried out by LGC Genomics (LGC Genomics GmbH, Berlin, Germany),
249 following the Ocean Sampling Day sequencing protocols from MicroB3 Project (Kopf et al. 2015).
250 Amplification of 16S rRNA gene fragment was performed using the primer pair 515F (5'-
251 GTGYCAGCMGCCGCGGTAA-3') (Caporaso et al. 2012) and the recently revised 926R (5'-
252 CCGYCAATTYMTTTRAGTTT-3') (Parada et al. 2016) as part of the Earth Microbiome Project (Gilbert
253 and Knight 2014) to increase detection of SAR11. The PCRs included about 5 ng of DNA extract, 15
254 pmol of each forward and reverse primers in 20 µL volume of MyTaq buffer containing 1.5 units
255 MyTaq DNA Polymerase (Bioline) and 2 µL of BioStabII PCR Enhancer (Sigma). For each sample, the
256 forward and reverse primers had the same 10-nt barcode sequence. PCRs were carried out for 30
257 cycles using the following parameters: 2 min 96 °C predenaturation; 96 °C for 15 s, 50 °C for 30 s, 70
258 °C for 90 s. DNA concentration of amplicons of interest was determined by gel electrophoresis.
259 About 20 ng amplicon of each sample were pooled with the other samples carrying different
260 barcodes. The amplicon pools were purified with one volume AMPure XP beads (Agencourt) to
261 remove primer dimer and other small mispriming products, followed by an additional purification on
262 MinElute columns (Qiagen). About 100 ng of each purified amplicon pool DNA were used to
263 construct Illumina libraries using the Ovation Rapid DR Multiplex System 1-96 (NuGEN).
264 Sequencing was performed on an Illumina MiSeq using V3 chemistry (Illumina). Sequence depth was
265 about 40,000 read pairs (combined raw reads) per sample. Quantitative Insights Into Microbial
266 Ecology (QIIME) pipeline was used to filter the quality of paired-end reads, assign taxonomy and
267 calculate alpha diversity metrics of 16S rDNA amplicon data (Caporaso et al. 2010). The quality of
268 paired-end Illumina reads was filtered using the *split_libraries_fastq.py* script based on quality
269 (Phred) scores per-nucleotide provided in the fastq files (MacQIIME v. 1.9.1). The quality parameters

270 chosen are the default as recommended by Bokulich et al. (2013). An exception was made to the
271 minimum Phred quality score - *q*=20 - in order to retrieve the bases with more than 99 % base call
272 accuracy. Then the chimeric sequences were identified based on reference database, the chimera-
273 free Greengenes (latest version - August 2013) database (DeSantis et al. 2006), and *de novo* based
274 on their abundances with usearch61 (v. 6.1.544 beta) wrapper in QIIME (Edgar 2010; (Navas-Molina
275 et al. 2013), that integrates the UCHIME algorithm (Edgar et al. 2011), and removed using the
276 following commands: *identify_chimeric_seqs.py* and *filter_fasta.py*. The preprocessed sequences
277 were clustered together into Operational Taxonomic Units (OTUs), taxonomy assigned and
278 phylogenetic tree built with *pick_open_reference_otus.py* script. The open reference approach was
279 chosen to pick OTUs in order to yield greater diversity in less time. This was achieved using
280 usearch61 (v. 6.1.544 beta), a centroid-based clustering algorithm, wrapped in QIIME. The most
281 abundant OTU within each cluster was picked as a representative sequence to be taxonomically
282 assigned to one reference sequence within the Greengenes 16S rRNA gene database through the
283 default QIIME-based wrapper classifier, the RDP naive Bayesian classifier (Wang et al. 2007b). The
284 representative OTUs that did not have similarity with any reference sequence were assigned as new
285 reference sequences and included in the database. OTUs with one sequence (singletons) were
286 excluded from built OTU table. The OTU tables at phylum and order levels were obtained with the
287 *core_diversity_analysis.py* command being rarefied at 18433 reads. Also, the alpha diversity metrics
288 (within samples), Chao1 estimator, Shannon and Good's coverage, were estimated from the OTU
289 table, already rarefied, using the *alpha_diversity.py* script in MacQIIME (v. 1.9.1).
290

291 **2.9. Nucleotide Sequence Accession Numbers**

292 The Illumina MiSeq raw reads have been deposited in the NCBI Sequence Read Archive (SRA)
293 database under the Bioproject PRJNA374525.
294

295 **2.10. PICRUSt functional predictions**

296 An *in silico* based approach using PICRUSt (Phylogenetic Investigation of Communities by
297 Reconstruction of Unobserved States) software (Langille et al. 2013) was used to predict the
298 metagenome of the microbial communities associated with the different microcosm treatments
299 based on 16S rDNA amplicon sequences. PICRUSt, using an extended ancestral-state reconstruction
300 algorithm, assigns gene families to the provided 16S rDNA sequences classified based on
301 phylogenetic proximity to reference genes with available genomes (Langille et al. 2013).
302 Functional traits of microbial communities associated with each treatment were inferred using
303 PICRUSt software. OTUs were picked using a *pick_closed_reference_otus.py* command from

304 MacQIIME (v. 1.9.1) with greengenes database (Caporaso et al. 2010). The frequency of each OTU
305 was normalized from the OTU table dividing the observed 16S rDNA amplicons by the 16S rRNA gene
306 copy numbers predicted: *normalize_by_copy_number.py* (PICRUSt v. 1.1.0). The functional profile
307 was traced multiplying each normalized OTU by each functional gene predicted using KEGG (Kyoto
308 Encyclopedia of Genes and Genomes) Orthology (Kanehisa et al. 2000) as annotation reference
309 database: *predict_metagenomes.py* (PICRUSt). Some genes are represented in multiple pathways, so
310 we used the *categorize_by_function.py* script to summarize the predictions at the level of the
311 individual pathways.
312 The relative abundance of predicted genes involved in denitrification and DNRA processes, and in
313 PAH degradation pathway was analyzed. KEGG Orthology (KOs) related with genes of denitrification
314 and DNRA pathways were assessed, namely: K00370 (*narG*), K00371 (*narH*), K00374 (*narI*), K00373
315 (*narJ*), K02567 (*napA*), K02568 (*napB*), K00362 (*nirB*), K00363 (*nirD*), K03385 (*nrfA*), K00368 (*nirK*),
316 K04561 (*norB*), K02305 (*norC*), K00376 (*nosZ*). In addition to this, KOs related with genes encoding
317 enzymes that might be involved in the aerobic: K00449 (*pcaH*), K00448 (*pcaG*), K14579 (*nahAc*,
318 *ndoB*, *nbzAc*, *dntAc*), K14580 (*nahAd*, *ndoC*, *nbzAd*, *dntAd*), K14578 (*nahAb*, *nagAb*, *ndoA*, *nbzAb*,
319 *dntAb*), K14583 (*nahC*), K05549 (*banA*), K14570 (*etbAc*); and anaerobic: K07540 (*bssA*), K07539
320 (*bamA*, *oah*), K04114 (*bcrA*), K04112 (*bcrC*), K07543 (*bbsE*), K07544 (*bssF*), K10700 (*ebdA*), K04109
321 (*hcrB*), K04105 (*hbaA*) degradation of PAHs were also assessed.
322

323 ### 2.11. Statistical analyses

324 Initial sediment samples were analyzed in triplicate for all relevant parameters (OM, water content,
325 TVCs, denitrification activity, and hydrocarbon concentration). Mean and standard deviations values
326 were calculated in triplicate for all parameters. Significant differences ($P < 0.05$) between L1 and L3
327 for relevant parameters were evaluated using *t*-tests. Differences on naphthalene, fluoranthene,
328 NH_4^+, NO_3^-, NO_2^-, and denitrification activity among treatments were analyzed by a parametric one-
329 way analysis of variance (ANOVA). If a significant ($P < 0.05$) difference was detected, a multiple
330 Tukey comparison test was performed to find out where the difference was. All statistical tests were
331 performed using the commercial software STATISTICA, version 7, StatSoft, Inc. (2004). Heatmaps and
332 Spearman correlation were generated using Hmisc, corrplot and ggplot2 packages in R (Harrell and
333 Harrell 2015; Wei 2013; Wickham 2009, respectively).
334

335 ## 3. Results and Discussion

336 ### 3.1. Sediment characterization and potential of indigenous microorganisms for
337 nitrate reduction

338 Sites L1 and L3 differed significantly in terms of physical and chemical sediment characteristics, *in-*
339 *situ* denitrification rates and natural PAH levels (Table 1). Site L1 was sandy and mostly consisted of
340 coarse medium sized (0.25–1 mm) sand particles, while site L3 was clayey and rich in silt with
341 significantly higher (*t*-test, $P < 0.05$) organic matter and water content. Sediment characteristics can
342 influence the nutrient content including carbon substrate and surface area available for microbial
343 colonization, which in turn reflects the growth, size, and structure of microbial populations and
344 therefore may enforce varying biogeochemical processes (reviewed by Dang and Lovell 2016). In
345 fact, fine muddy textured and compressed sediments (similar to the L3 site) are prone to anoxic
346 conditions due to restricted air exchange and oxygen diffusion (Gingras et al. 2014; Horn et al. 1994).
347 Moreover, a disparity was observed in the *in situ* denitrification activity at both sites (Table 1).
348 Conspicuously higher (*t*-test, $P < 0.05$) denitrification rates were established at L3 compared to L1
349 which may be attributed to rich organic matter and prevalence of anaerobic conditions in L3
350 sediments (De Sousa and Bhosle 2012). Total viable counts of the native L1 and L3 communities
351 were estimated on NRM and BTB plates and, as expected, results showed higher (*t*-test, $P < 0.05$)
352 bacterial counts on NRM (approaching 10^5 CFU mL^{-1}) compared to BTB (in the vicinity of 10^3 CFU mL^{-}
353 ^{1}) from both L1 and L3 (Table 1). More blue haloed colonies were obtained from L1 (253 colonies)
354 sediments compared to L3 (23 colonies), indicating a predominance of dissimilatory nitrate reducers
355 in L1 than L3, since BTB medium is specially designed to enrich denitrifying bacteria and also bacteria
356 capable of DNRA (Takaya et al. 2003).
357 High levels of total petroleum hydrocarbons (TPHs) including the 16 EPA PAHs (757.71 µg kg^{-1} of
358 sediment) were found at site L3, probably due to the higher organic matter content and small grain
359 size of these sediments (Ribeiro et al. 2011, Ribeiro et al. 2013a). Furthermore, significantly higher
360 levels (*t*-test, $P < 0.05$) of naphthalene (28.58 µg kg^{-1} of sediment) and fluoranthene (96.69 µg kg^{-1} of
361 sediment) were obtained in L3 sediments. On the other hand, relatively lower levels of naphthalene
362 (19.09 µg kg^{-1} of sediment) and fluoranthene (3.78 µg kg^{-1} of sediment) were found at site L1. Clay
363 minerals and OM content can play a critical role in hydrocarbon biodegradation processes by
364 positively influencing the absorption and sequestration of hydrocarbons (Scherr et al. 2007; Ribeiro
365 et al. 2013a).
366

367 **3.2. PAH degradation in laboratory designed microcosms**

368 Naphthalene is a semi-volatile organic compound (vapor pressure: 11.8 Pa) and soluble in water
369 (solubility: 31.6 mg L^{-1} at 25 °C) (Bojes and Pope 2007). Loss of naphthalene (less than 40 % of that
370 originally added remained) at the beginning of the incubation, detected in L1 microcosms (Figure
371 1A), might be attributed to volatilization losses during sampling at the end of each time period.

372 Although, we were unable to actually quantify the contribution of biodegradation to the removal of
373 naphthalene in the L1 microcosms during the incubation period; it seemed that the reduction of
374 naphthalene in L1 sediments and in respective liquid medium is abiotic, since the same tendency
375 occurred in autoclaved controls after 63 weeks of incubation.
376 On the other hand, in L3 sediments (higher OM content) and in the liquid medium, we detected ca.
377 60 % of the naphthalene added (Figure 1B), 88 % of this compound quota incorporated in sediments.
378 These observations reflected the higher hydrocarbon adsorption capacity of the L3 sediments (Chen
379 et al. 2004). However, the higher sorption of naphthalene onto OM contents and clay particles does
380 not seem to affect their bioavailability for microbial degradation (Meredith and Radosevich 1998). In
381 fact, a significant (ANOVA, $P < 0.05$) depletion (around 50 % compared to initial levels) of
382 naphthalene in L3 sediments was seen at 6, 12, 30 and 63 weeks, and approximately 35 % was
383 biologically degraded compared to the control. It is most likely that in L3 sediments, the abiotic
384 losses of naphthalene (15 %) were also due to volatilization into head-space and losses during
385 sampling.
386 Due to the lower vapor pressure (0.00108 Pa) and solubility (0.26 mg L^{-1} at 25 °C) (Bojes and Pope
387 2007), fluoranthene is less volatile and soluble in water than naphthalene and is not expected to be
388 in liquid and gas-phase at room temperatures. In fact, 99.7 % of fluoranthene was accounted for in
389 L1 sediments and only 0.3 % in liquid medium (Figure 1C). The same trend occurred in L3 sediments
390 (99.4 % of total fluoranthene), with only 0.6 % in the liquid medium (Figure 1D). Significant (ANOVA,
391 $P < 0.05$) fluoranthene biological degradation (around 50 %, on an average, compared to autoclaved
392 control sediments) was found after 63 weeks in L1 sediments (Figure 1C), without significant
393 (ANOVA, $P > 0.05$) abiotic degradation found in the autoclaved sediments. A significant (ANOVA, $P <$
394 0.05) fluoranthene biological degradation (around 30 % compared to autoclaved sediments) in L3
395 sediments (Figure 1D) was seen at 6, 30 and 63; and average abiotic losses of 10 % (autoclaved
396 sediments).
397 Naphthalene comprises two benzene rings and is generally more susceptible to microbial
398 degradation compared to PAHs with higher molecular weight like fluoranthene, which has four rings
399 including 3 benzene rings (Chikere et al. 2011). Consistent with this, L3 sediments showed slightly
400 higher naphthalene (35 %) than fluoranthene (30 %) biodegradation.
401 It has been shown that the rates of anaerobic degradation are typically lower than under aerobic
402 conditions (McNally et al. 1998). Although the actual denitrification reaction is anaerobic, the
403 breakdown of organic matter under denitrifying conditions may not completely exclude the role of
404 oxygen especially in the initial breakdown reactions (Chayabutra and Ju 2000). Studies have shown
405 that efficient breakdown of recalcitrants pollutants, including PAHs, under anaerobic denitrifying

406 conditions employ trace oxygen for the initial ring cleavage before proceeding to the complete
407 breakdown via anaerobic processes (Wilson and Bouwer 1997; Yerushalmi et al. 2001). This is a
408 more viable phenomenon in the prevailing environments since oxygen may be produced by
409 anaerobic nitrate respiration, through disproportionation of the NO (Ettwig et al. 2010). In fact,
410 disproportionation of the NO is catalyzed by a putative NO dismutase (Nod) with widespread
411 occurrence and diversity in the aromatic hydrocarbons contaminated aquifers and nitrogen
412 removing wastewater treatment systems (Zhu et al. 2017). Therefore, caution should be taken on
413 the interpretation of PAHs degradation results, including those presented in this study, since the
414 initial PAHs degradations under nitrate reducing conditions can be due to aerobic or microaerophilic
415 pathways. Nevertheless, the removal percentages in the present study were lower than those
416 reported by other studies under anaerobic conditions using pure strains (McNally et al. 1998; Rockne
417 et al. 2000) or microbial consortia (Ambrosoli et al. 2005; Chang et al. 2001; Chang et al. 2002).
418

419 **3.3. Nitrogen biogeochemistry under dissimilatory nitrate-reducing conditions**

420 The nitrogen cycle contains two different processes of dissimilatory nitrate (NO_3^-) reduction,
421 denitrification, and DNRA. In order to monitor the progress of these complex microbial reactions of
422 the intricate nitrogen cycle, NH_4^+, NO_2^-, NO_3^-, N_2O and N_2 production/removal were measured over
423 63 weeks in L1 (Table 2) and L3 (Table 3) sediments spiked with naphthalene and fluoranthene, and
424 the un-amended with PAHs control treatment.
425 In L1 sediments there was NO_3^- consumption during the 63 weeks incubation period. This result was
426 maximum after 63 weeks, with significant (ANOVA, $P < 0.05$) NO_3^- consumption compared to the
427 initial (week 0) and to autoclaved controls (Table 2), indicating activity of the nitrate reducers. There
428 was also a tendency for an increase (ANOVA, $P < 0.05$) of NH_4^+ levels over time compared to the
429 initial (week 0), particularly at 30 and 63 weeks; however, without significant differences (ANOVA, P
430 > 0.05) compared to autoclaved control NH_4^+ concentrations. Nevertheless, the contribution of DNRA
431 populations cannot be disregarded, since the autoclave process can increase ammonium levels
432 (Trevors 1996). Under anaerobic conditions, N_2O is the penultimate product (last intermediate)
433 before the final end product (N_2), of denitrification (Tiedje 1988). Therefore both (N_2O and N_2) can
434 be used to evaluate denitrification potential. Minor N_2O production rates fluctuations in control L1
435 sediments suggest that denitrifiers were not affected (positively or negatively) by the experimental
436 conditions. Lower or zero N_2O or/and N_2 production rates was detected in autoclaved controls.
437 Remarkably, N_2O production rates (Table 2) increased (ANOVA, $P > 0.05$) in L1 sediments spiked with
438 fluoranthene (after 30 and 63 weeks) and naphthalene (after 63 weeks).

In L3 sediments, NO_3^- consumption was significant (ANOVA, $P < 0.05$), even verified after 3 weeks; and more rapid than that observed in L1 sediments. Our findings suggest an activation of the NO_3^- reduction processes over time in response to NO_3^- availability in L3 sediments. N_2O and/or N_2 production rates increased steadily over a period of 63 weeks in L3 sediments. The absence, in L3 sediments, of N_2O and/or N_2 production rates at week 30 is consistent with NO_3^- limitation registered at this period of incubation (Table 3). Additionally, no significant differences were found between NO_3^- levels at the start of the incubation period (0 weeks) and autoclaved controls (after 63 weeks). These results indicate an active involvement of the nitrate reducers in the NO_3^- consumption process and an absence of abiotic consumption. Moreover, N_2O and N_2 production rates were significantly higher (ANOVA, $P < 0.05$) than those found in L1 sediments. Therefore, denitrifiers seemed to have a fundamental role in NO_3^- reducing process in L3 sediments. However, many microorganisms conducting DNRA also produce N_2O as a detoxification mechanism in order to avoid high concentrations of NO_2^- (Cole 1988; Rütting et al. 2011). However, the N_2O production rate by DNRA microorganisms is typically in the low range of 1 % of the NO_2^- or NO_3^- reduction (Cole 1988). Additionally, there was a tendency for an increase (ANOVA, $P < 0.05$) of the NH_4^+ levels with incubation time, particularly after the 63 weeks incubation period (Table 3), which along with the tendency of NO_3^- consumption over time indicated an active involvement of the DNRA process in L3 sediments.

The absence of N_2O production rates in autoclaved sediments, the increase of N_2O or/and N_2 production and the NO_3^- disappearance in L1 and L3 sediments spiked with fluoranthene suggest that both fluoranthene degradation (Figure 1C and 1D) and denitrification are occurring concomitantly. This is in agreement with previous studies that have already shown the degradation of lower molecular weight PAHs under nitrate reducing conditions with the direct involvement of denitrifying communities (Mihelcic et al. 1988; Dou et al. 2009). Also, Interestingly, Dong et al. (2009) suggested that while decreasing nitrate concentrations debilitated denitrification, it boosted the potential for DNRA. Thus, the increase of NH_4^+ at and after week 12 in sediments spiked with naphthalene and fluoranthene, together with the high rates of NO_3^- consumption, can also suggest an active involvement of DNRA communities (Knowles 1982; Zumft 1997; Rütting et al. 2011). During the same period, naphthalene and fluoranthene degradation in L3 sediments is observed, and might be coupled with DNRA process.

3.4. Shifts in microbial communities

From a sequence input of 630903 pair reads, 460013 passed the quality filtering steps and chimera removal, with an open reference classified sequences of 95.71 %. The number of sequences was

473 rarefied to 18433 reads per sample for further analysis. The Illumina sequencing dataset is
474 summarized in Supplementary Table 1.
475 The most relevant information was given by the distribution of the OTUs in the different samples
476 since it corresponded to differences in their genetic structure as a function of the characteristics of
477 the sediments, naphthalene and fluoranthene contamination, and/or incubation period. Our results
478 showed a drastic difference in prokaryotic communities between the two sampling locations, L1 and
479 L3 (Figure 2). All samples had Good's coverage between 0.91-0.97 (Supplementary Table 1),
480 indicating sufficient sequencing depth to characterize bacterial diversity. Hierarchical cluster analysis
481 of the relative abundance of the occurrence of taxa at the phylum level grouped all analyzed DNA
482 samples, in two different clusters (Figure 2). Clustering separated sediments from L1 and L3, and the
483 second highest level of differentiation was incubation period (12 weeks and 63 weeks).
484 Concomitantly, the number of OTUs among all samples decreased with time of incubation, and the
485 differences could be detected even at the Phylum level (Supplementary Table 1). In agreement,
486 Shannon and Chao1 indices revealed higher OTUs diversity and richness after 12 weeks than after 63
487 weeks, in both sediments. These results clearly indicate that the original type of sediment (L1 or L3),
488 or/and sediment characteristics, may act as a major selection factor for prokaryotic assemblage. This
489 is in agreement with other studies showing that sediment characteristics are a more important
490 factor than hydrocarbon contamination for determining bacterial community structure (Hamamura
491 et al. 2006; Ribeiro et al. 2015). Also, the enrichment over time also acts as a differentiating factor
492 for prokaryotic assemblage.
493 A closer analysis revealed an increase in the relative abundance of certain phyla in treatments with
494 naphthalene and fluoranthene compared to the treatments without PAH (Supplementary Figure 1).
495 These results further suggested that both PAHs affected specific prokaryotic populations at a higher
496 taxonomic rank, which is consistent with other studies (Yang et al. 2014). In L1 sediments the
497 number of OTUs and the alpha diversity indices (Shannon and Chao1) decreased to a greater extent
498 (57 % average loss) than L3 sediments (27 % average loss) after 63 weeks of incubation. This
499 tendency was registered also at Family, Order, Class and Phylum level (Supplementary Table 1).
500 Thus, a higher effect of the experimental design in L1 sediments was observed probably due to the
501 different geochemical characteristics on L1 and L3 (Table 1), since higher strict aerobic communities
502 are expected in more oxygenated sediments (L1), which may be more affected in incubations under
503 anoxic conditions.
504

505 **3.5. PAH and N genes *in silico* analysis, using PICRUSt**

506 Recent molecular biology techniques, and *in silico* analysis of metagenomes, provide an opportunity

507 to predict functional content, and therefore an understanding of the microbial hydrocarbon
508 degradation processes (Langille et al. 2013). PICRUSt analysis shows an increase in the relative
509 abundance of several KOs involved in aerobic PAHs degradation pathways (Figure 3) in L1 sediments
510 with naphthalene and fluoranthene compared to controls. This result is particularly evident, after 12
511 weeks, for the observed genes encoding the alpha subunit of naphthalene 1,2-dioxygenase enzyme
512 (*nahAc*, *ndoB*, *nbzAc* and *dntAc*), which play a critical role in initiating the degradation of
513 naphthalene and low-molecular-weight PAHs (Mallick et al. 2011). In addition, in L1 sediments, the
514 genes *nahC*, *banA*, *etbAc*, and *pcaH* involved in PAHs aerobic degradation pathways also increased in
515 naphthalene and fluoranthene treatments.
516 An increase in the relative abundance of genes involved in anaerobic PAHs degradation could also be
517 predicted in spiked L1 sediments (*bamA*, *bcrC*, *bcrA* in naphthalene treatment; and *bssA*, *bssF*, *bbsE*
518 in fluoranthene treatment) (Figure 3). The *bssA* gene encoding the alpha subunit of benzylsuccinate
519 synthase enzyme has been identified as being responsible for the first step of anaerobic toluene
520 metabolism (Carmona et al. 2009; Heider et al. 2016). After 63 weeks, the anaerobic catabolic PAHs
521 genes were higher in sediments spiked with fluoranthene than naphthalene and control. Clearly, it
522 seems that microbial communities from L1 sediments spiked with naphthalene and fluoranthene
523 develop mechanisms and adapt their metabolic pathways to PAHs degradation, as suggested in
524 previous studies (Van Hamme et al. 2003; Chikere et al. 2011).
525 Spearman correlations for L1 sediments (Figure 4) revealed a strong degree of interrelation between
526 some KOs of genes involved in aerobic and anaerobic degradation and those of nitrate reducing
527 pathways. Positive relations between the relative abundance of genes related to aerobic PAHs
528 degradation (*nahC* and *banA*) and the genes involved in NO_3^- reduction to NO_2^- (respectively, *narI*,
529 *narJ*) and in NO_2^- reduction to NO (*nirK*, gene) were registered. On the other hand, a negative
530 correlation was found between aerobic degradation genes (*nahC* and *banA*) and *nrfA* gene involved
531 in DNRA pathway. These results point that, in L1 sediments, aerobic PAHs degradation might be
532 coupled with denitrification, which may occur under microaerophilic conditions as suggested
533 previously in Section 3.2.
534 Regarding the genes involved in anaerobic degradation, Spearman correlations results for L1
535 sediments shows negative correlations with genes involved in denitrification; and positive
536 correlations with DNRA genes (Figure 4). Interestingly, a positive relation between genes involved in
537 the DNRA pathway of NO_2^- reduction to NH_4^+, (*nirD*, and *nrfA*) and the genes involved in anaerobic
538 PAHs degradation (*bssA*, *bbsE*, *bssF* and *hcrB*) was observed. The possibility of microbial populations
539 that anaerobically consume aromatic compounds and carry out coupled cycling of nitrogen via DNRA
540 was reported by Yagi et al. (2010) showing *bssA* and *nrfA* genes transcription in a contaminated site.

541 Despite this result, aromatic compounds were only metabolized under oxic conditions in laboratory
542 experiments (Yagi et al. 2010). Weekly and/or negative correlation was found between aerobic and
543 anaerobic PAH degradation genes at L1, suggesting independence of the aerobic and anaerobic PAH
544 degradation metabolic pathways.
545 In the muddy samples (L3 sediments), PICRUSt results showed a higher proportion of majority of the
546 genes involved in the nitrate dissimilatory metabolism at week 63 (Figure 5), particularly in
547 sediments spiked with naphthalene. It seemed that communities actively responded to both PAHs
548 additions by increasing the frequency of *nahAc*, *nahC*, *banA*, *etbAc*, *pcaH*, *pcaG* in L3 sediments
549 spiked with naphthalene and *pcaH*, *pcaG* genes in sediments with fluoranthene (Figure 5). Also, a
550 predicted higher relative abundance of the genes involved in anaerobic PAHs degradation,
551 particularly *bssA*, *bssF*, *bbsE*, *bamA*, *bcrC*, *bcrA*, *ebdA*, and *hcrB* was seen in the at 63 weeks
552 sediments spiked with naphthalene (Figure 5). In sediments spiked with fluoranthene, only *bamA*,
553 *bcrC*, and *bcrA* genes increased relative to the controls.
554 High degree of positive interrelationships between the genes involved in nitrate reduction and
555 aerobic and anaerobic PAH degradation pathways were registered at L3, which suggests the
556 involvement of nitrate reducers in the degradation of naphthalene and fluoranthene. In fact, the
557 denitrification activity and NH_4^+ (eventually produced by DNRA) increased (Table 3), together with
558 significant decrease in both PAHs (Figure 1B and 1D). This reinforced the hypothesis that anaerobic
559 naphthalene and fluoranthene degradation might be coupled with DNRA and denitrifying processes
560 in L3 sediment.
561 The *in silico* prediction of functional potential reflects to some extent species composition and
562 represents an important resource to evaluate shifts in the potential bacterial traits between the
563 different treatments (Langille et al. 2013, Lindgreen et al. 2016). However, genes coding for the
564 catabolism of PAH enzymes are also found in mobile genetic elements, such as transposons and
565 plasmids (Wilson et al. 2003; Yuan et al. 2017), therefore, the *in silico* analysis based on the 16S
566 rRNA gene does not necessarily fully predict catabolic potential.
567 The extrapolation of the results of microbial PAH biodegradation performed in laboratory designed
568 experiments to the environment may be limited. It may not be feasible to mimic and control several
569 factors and environmental conditions in a laboratory design which may be crucial to the degradation
570 pathways of PAHs (Varjani 2017). Nonetheless, the collective results reiterate the intervention of
571 denitrifying and DNRA communities in tested PAHs degradation with a strong influence of PAHs on
572 the metabolic activities of the indigenous microbial communities. Although, we believe that the
573 results from this investigation are emphatic and will significantly contribute to understand the
574 nitrogen anaerobic pathways involved in degradation of naphthalene and fluoranthene.

575 # 4. Conclusion

576 This study demonstrated a decrease in naphthalene and fluoranthene over time with distinct
577 degradation dynamics varying with the sediment type. In fact, original sediment type seemed to be a
578 major driver on the shifts of microbial consortia observed between the different treatments.
579 Denitrification signals, NO_3^- consumption and an NH_4^+ increase, and predicted microbial functional
580 data analyses clearly suggested the involvement of the dissimilatory nitrate-reducing pathways
581 (denitrification and DNRA) in the degradation of naphthalene and fluoranthene. We believe that our
582 study may shed some light to the relationship between dissimilatory nitrate-reducing pathways and
583 microbial community shifts involved in PAH degradation. These results will be helpful for directing
584 remediation strategies of the PAH-contaminated anoxic sites.

585

586 **Author Contributions**

587 HR, TS and CM conceived, designed and performed the experiments, analyzed all data and wrote the
588 manuscript. CT, CMRA and APM performed PAHs analyses. HR and PS performed denitrification
589 analyses. JS performed nutrient analyses. HR performed statistical analyses. LT developed R pipeline
590 for NGS data analysis. MM, AGGS, LT and CM performed and analyzed the NGS data.

591

592 **Acknowledgement**

593 The authors acknowledge the reviewers for their valuable comments and suggestions, which were
594 helpful in improving the manuscript. This research was partially supported by the Structured
595 Program of R&D&I INNOVMAR - Innovation and Sustainability in the Management and Exploitation
596 of Marine Resources. The post-doctoral scholarship granted by Erasmus Mundus Interweave to T. de
597 Sousa is greatly acknowledged. C. Magalhães acknowledges Investigator FCT program supported by
598 FCT, funded by the European Social Fund through the Operational Program of Human Capital
599 (POCH). C. Teixeira acknowledges FCT for a postdoctoral grant (ref. SFRH/BPD/110730/2015)
600 cofunded by MCTES and the European Social Fund through POCH/QEC.

601

602 **References**

603 Ambrosoli, R., Petruzzelli, L., Minati, J.L., Marsan, F.A., 2005. Anaerobic PAH degradation in soil by a
604 mixed bacterial consortium under denitrifying conditions. Chemosphere 60, 1231-1236.
605 Atlas, R.M., Parks, L.C., 1997. Handbook of Microbiological media, 2d ed. CRC Press Inc., USA
606 Bojes, H.K., Pope, P.G., 2007. Characterization of EPA's 16 priority pollutant polycyclic aromatic
607 hydrocarbons (PAHs) in tank bottom solids and associated contaminated soils at oil exploration
608 and production sites in Texas. Reg. Toxicol. Pharmacol. 47, 288-295.

Bokulich, N.A., Subramanian, S., Faith, J.J., Gevers, D., Gordon, J.I., Knight, R., et al., 2013. Quality-filtering vastly improves diversity estimates from Illumina amplicon sequencing. Nat. Methods 10, 57-59.

Cao, B., Nagarajan, K., Loh, K., 2009. Biodegradation of aromatic compounds: current status and opportunities for biomolecular approaches. Appl. Microbiol. Biotechnol. 85, 207-228.

Caporaso J.G., Walters, W.A., Berg-Lyons, D., Huntley, J., Fierer, N., Owens, S.M., et al., 2012. Ultra-high-throughput microbial community analysis on the Illumina HiSeq and MiSeq platforms. ISME J. 6, 1621-1624.

Caporaso, J.G., Kuczynski, J., Stombaugh, J., Bittinger, K., Bushman, F.D., Costello, E.K., et al., 2010. QIIME allows analysis of high-throughput community sequencing data. Nat. Methods 7, 335-336.

Carmona, M., Zamarro, M.T., Blazquez, B., Durante-Rodriguez, G., Juarez, J.F., Valderrama, J.A., et al., 2009. Anaerobic Catabolism of Aromatic Compounds: a Genetic and Genomic View. Microbiol. Mol. Biol. Rev. 73: 71.

Chang, B.V., Shiung, L.C., Yuan, S.Y., 2002. Anaerobic biodegradation of polycyclic aromatic hydrocarbon in soil. Chemosphere 48, 717–724.

Chang, B.V., Chang, J.S., Yuan, S.Y., 2001. Degradation of phenanthrene in river sediment under nitrate-reducing conditions. Bull. Environ. Contam. Toxicol. 67, 898–905.

Chauhan, A., Fazhurrahman, Oakeshott, J.G., Jain, R.K., 2008. Bacterial metabolism of polycyclic aromatic hydrocarbons strategies for bioremediation. Indian J. Microbiol. 48, 95-113.

Chayabutra, C., and Ju, L., 2000. Degradation of n-hexadecane and its metabolites by *Pseudomonas aeruginosa* under microaerobic and anaerobic denitrifying conditions. Appl. Environ. Microbiol. 66, 493-498.

Chen, B., Xuan, X., Zhu, L., Wang, J., Gao, Y., Yang, K., et al., 2004. Distributions of polycyclic aromatic hydrocarbons in surface waters, sediments and soils of Hangzhou city, China. Water Res. 38, 3558-3568.

Chikere, C.B., Okpokwasil, G.C. Chikere, C.O., 2011. Monitoring of microbial hydrocarbon remediation in the soil. 3 Biotech 1, 117-138.

Cole, J.A., 1988. Assimilatory and dissimilatory reduction of nitrate to ammonia, in: Cole, J.A., Ferguson S.J. (Eds.), The Nitrogen and Sulphur Cycles. Cambridge University Press, Cambridge, pp. 281–329.

Dang, H., Lovell, C.R., 2016. Microbial surface colonization and biofilm development in marine environments. Microbiol. Mol. Biol. Rev. 80, 91–138.

De Sousa, T., 2015. Denitrifying bacteria: Physiological response to hydrocarbons, in: Borkar S. (Eds.), Bioprospects of Coastal Eubacteria. Springer International Publishing, pp. 39-57.

De Sousa, T., Bhosle, S., 2012. Microbial denitrification and its ecological implications in the marine system, in: Satyanarayana, T., Johri, B.N., Prakash, A. (Eds.), Microbes in environmental management. Springer, pp. 683-700.

DeSantis, T.Z., Hugenholtz, P., Larsen, N., Rojas, M., Brodie, E.L., Keller, K., et al., 2006. Greengenes, a chimera-checked 16S rRNA gene database and workbench compatible with ARB. Appl. Environ. Microbiol. 72, 5069-5072.

Dong, L.F., Smith, C.J., Papaspyrou, S., Stott, A., Osborn, A.M., Nedwell, D.B., 2009. Changes in benthic denitrification, nitrate ammonification, and anammox process rates and nitrate and nitrite reductase gene abundances along an estuarine nutrient gradient (the Colne Estuary, United Kingdom). Appl. Environ. Microbiol. 75, 3171-3179.

Dou, J., Liu, X., Ding, A., 2009. Anaerobic degradation of naphthalene by the mixed bacteria under nitrate reducing conditions. J. Hazard. Mater. 165, 325-331.

Edgar, R.C., 2010. Search and clustering orders of magnitude faster than BLAST. Bioinformatics 26, 2460-2461.

Edgar, R.C., Haas, B.J., Clemente, J.C., Quince, C., Knight, R., 2011. UCHIME improves sensitivity and speed of chimera detection. Bioinformatics 27, 2194-2200

Ettwig, K.F., Butler, M.K., Le Paslier, D., Pelletier, E., Mangenot, S., Kuypers, M.M.M., et al., 2010. Nitrite-driven anaerobic methane oxidation by oxygenic bacteria. Nature 464, 543–548.

Ghattas, A.K., Fischer, F., Wick, A., Ternes, T.A., 2017. Anaerobic biodegradation of (emerging) organic contaminants in the aquatic environment. Water Res. 116, 268-295.

Gilbert, J.A., Knight, R., 2014. The Earth Microbiome project: successes and aspirations. BMC Biology 12(1): p. 69.

Gingras, M., Pemberton, S. G., Smith, M., 2014. Bioturbation: reworking sediments for better or worse. Oilfield Rev. 26, 46-58.

Gonçalves, C., Teixeira, C., Basto, M.C.P., Almeida, C.M.R., 2016. PAHs levels in Portuguese estuaries and lagoons: salt marsh plants as potential agents for the containment of PAHs contamination in sediments. Reg. Stu. Mar. Sci. 7, 211-221.

Grasshoff, K., Ehrhardt, M., Kremling, K., 1983. Methods of Seawater Analysis. Verlag Chemie. Weinheim.

Hamamura, N., Olson, S., Ward, D., Inskeep, W., 2006. Microbial population dynamics associated with crude-oil biodegradation in diverse soils. Appl. Environ. Microbiol. 72: 6316–6324.

Harrell, Jr F.E., Harrell, Jr M.F.E., 2015. Package 'Hmisc'.

Head, I.M., Jones, D.M., Roling, W.F.M., 2006. Marine microorganisms make a meal of oil. Nat. Rev. Microbiol. 4, 173–182.

677 Heider, J., Szaleniec, M., Martins, B. M., Seyhan, D., Buckel, W., Golding, B.T., 2016. Structure and
678 function of benzylsuccinate synthase and related fumarate-adding glycyl radical enzymes. J. Mol.
679 Microbiol. Biotechnol. 26, 29-44.
680 Horn, R., Taubner, H., Wuttke, M., Baumgartl, T., 1994. Soil physical properties related to soil
681 structure. Soil Till. Res. 30, 187–216.
682 Jain, R.K., Gupta, V.K., Gaur, R.K., Lowry, M., Jaroli, D.P., Chauhan, U.K., 2011. Bioremediation of
683 petroleum oil contaminated soil and water. Res. J. Environ. Toxicol. 5, 1-26.
684 Jones, M.N., 1984. Nitrate reduction by shaking with cadmium: alternative to cadmium columns.
685 Water Res. 18, 643–646.
686 Joye, S.B., Teske, A.P., Kostka, J.E., 2014. Microbial dynamics following the Macondo oil well blowout
687 across Gulf of Mexico environments. BioScience 64, 766-777.
688 Joye, S. B., Kleindienst, S., Gilbert, J.A., Handley, K.M., Weisenhorn, P., Overholt, W.A., Kostka, J.E.,
689 2016. Responses of microbial communities to hydrocarbon exposures. Oceanography 29, 136–
690 149.
691 Kanehisa, M., Goto S., 2000. KEGG: kyoto encyclopedia of genes and genomes. Nucleic Acids Res. 28,
692 27–30.
693 Knowles, R., 1982. Denitrification. Microbiol. Rev. 46, 43-70.
694 Kopf, A., Bicak, M., Kottmann, R., Schnetzer, J., Kostadinov, I., Lehmann, K. et al., 2015. The ocean
695 sampling day consortium. Gigascience 4: 27.
696 Ladino-Orjuela, G., Gomes E., Silva R., Salt C., Parsons, J.R., 2016. Metabolic pathways for
697 degradation of aromatic hydrocarbons by bacteria, in: Voogt P. (Eds.), Reviews of Environmental
698 Contamination and Toxicology 237, Springer, pp. 105–121.
699 Langille, M.G.I., Zaneveld, J., Caporaso, J.G., McDonald, D., Knights, D., a Reyes, J., et al., 2013.
700 Predictive functional profiling of microbial communities using 16S rRNA marker gene sequences.
701 Nat. Biotechnol. 31, 814–21.
702 Lindgreen, S., Adair, K., Gardner, P., 2016. An evaluation of the accuracy and speed of metagenome
703 analysis tools. Sci. Rep. 6, 19233.
704 Magalhães, C., Joye, S.B., Moreira, R.M., Wiebe, W.J., Bordalo, A.A., 2005. Effect of salinity and
705 inorganic nitrogen concentrations on nitrification and denitrification rates in intertidal sediments
706 and rocky biofilms of the Douro River estuary, Portugal. Water Res. 39, 1783-1794.
707 Mallick S., Chakraborty J., Dutta T.K., 2011. Role of oxygenases in guiding diverse metabolic
708 pathways in the bacterial degradation of low-molecular-weight polycyclic aromatic
709 hydrocarbons: a review. Crit. Rev. Microbiol. 37, 64–90.

ACCEPTED MANUSCRIPT

McNally D.L., Mihelcic J.R., Lueking D.R., 1998. Biodegradation of three- and four-ring polycyclic aromatic hydrocarbons under aerobic and denitrifying conditions. Environ. Sci. Technol. 32, 2633–2639.

Meckenstock, R.U., Boll, M., Mouttaki, H., Koelschbach, J.S., Tarouco, P.C., Weyrauch, P., et al., 2016. Anaerobic degradation of benzene and polycyclic aromatic hydrocarbons. J. Mol. Microbiol. Biotechnol. 26, 92–118.

Meredith, C.E., Radosevich, M., 1998. Bacterial degradation of homo- and heterocyclic aromatic compounds in the presence of soluble/colloidal humic acid. J. Environ. Sci. Health B. 33, 17-36.

Mihelcic, J.R., Luthy, R.G., 1988. Microbial degradation of acenaphthene and naphthalene under denitrification conditions in soil-water systems. Appl. Environ. Microbiol. 54, 1188-1198.

Navas-Molina, J.A., Peralta-Sánchez, J.M., González, A., McMurdie, P.J., Vázquez-Baeza, Y., Xu, Z., et al., 2013. Advancing our understanding of the human microbiome using QIIME. Methods Enzymol. 531, 371-444

Parada, A.E., Needham, D.M., Fuhrman, J.A., 2016. Every base matters: assessing small subunit rRNA primers for marine microbiomes with mock communities, time series and global field samples. Environ. Microbiol. 18, 1403–1414.

Rabus, R., Boll, M., Heider, J., Meckenstock, R.U., Buckel, W., Einsle, O., et al., 2016. Anaerobic microbial degradation of hydrocarbons: from enzymatic reactions to the environment. J. Mol. Microbiol. Biotechnol. 26 5–28.

Rengarajan, T., Rajendran, P., Nandakumar, N., Lokeshkumar, B., Rajendran, P., Nishigaki, I., 2015. Exposure to polycyclic aromatic hydrocarbons with special focus on cancer. Asian Pac. J. Trop. Med. 5, 182-189.

Ribeiro, H., Almeida, C.M.R., Magalhães, C., Bordalo, A.A., Mucha, A.P., 2015. Salt marsh sediment characteristics as key regulators on the efficiency of hydrocarbons bioremediation by *Juncus maritimus* rhizospheric bacterial community. Environ. Sci. Pollut. Res. 22, 450-462.

Ribeiro, H., Mucha, A.P., Almeida, C.M.R., Bordalo, A.A., 2011. Hydrocarbon degradation potential of salt marsh plant-microorganisms associations. Biodegradation 22, 729 – 739.

Ribeiro, H., Mucha, A.P., Teixeira C., Almeida, C.M.R., Bordalo, A.A., 2013a. Influence of natural rhizosediments characteristics on hydrocarbons degradation potential of microorganisms associated to *Juncus maritimus* roots. Int. Biodeterior. Biodegrad. 84, 86-96.

Ribeiro H., Mucha A.P., Almeida C.M., Bordalo A.A., 2013b. Bacterial community response to petroleum contamination and nutrient addition in sediments from a temperate salt marsh. Sci. Total Environ. 458–460, 568–576.

743 Ribeiro, H., Mucha, A.P., Azevedo, I., Salgado, P., Teixeira, C., Almeida, C.M.R., Joye, S.B., Magalhães,
744 C., 2016. Differential effects of crude oil on denitrification and anammox, and the impact on N_2O
745 production. Environ. Pollut. 216, 391-399
746 Rockne K.J., Chee-Sanford J.C., Sandford R.A., Hedlund B.P., Staley J.T., 2000. Anaerobic naphthalene
747 degradation by microbial pure cultures under nitrate reducing conditions. Appl. Environ.
748 Microbiol. 66, 1595–1601.
749 Rütting, T., Boeckx P., Müller, C., Klemedtsson L., 2011. Assessment of the importance of
750 dissimilatory nitrate reduction to ammonium for the terrestrial nitrogen cycle. Biogeoscience 8,
751 1779-1791.
752 Scherr, K., Aichberger, H., Braun, R., Loibner, A.P., 2007. Influence of soil fractions on microbial
753 degradation behavior of mineral hydrocarbons. Eur. J. Soil Biol. 43, 341-350.
754 Takaya, N., Catalan-Sakairi, M.A.B., Sakagushi, Y., Kato, I., Zhou, Z., Shoun, H., 2003. Aerobic
755 denitrifying bacteria that produce low levels of nitrous oxide. Appl. Environ. Microbiol. 69, 3152-
756 3157.
757 Tiedje, J.M., 1988. Ecology of denitrification and dissimilatory nitrate reduction to ammonium, in:
758 Zehnder A.J.B. (Eds.), Biology of Anaerobic Microorganisms. John Wiley & Sons, New York, NY,
759 pp. 179-244.
760 Trevors, J., 1996. Sterilization and inhibition of microbial activity in soil. J. Microbiol. Methods 26,
761 53–59.
762 Varjani, S.J., Upasani, V.N., 2017. A new look on factors affecting microbial degradation of petroleum
763 hydrocarbon pollutants. Int. Biodeterior. Biodegrad. 120, 71-83.
764 Varjani, S.J., 2017. Microbial degradation of petroleum hydrocarbons. Bioresour. Technol. 223, 277-
765 286.
766 Van der Zaan, B.M., Saia, F.T., Stams, A.J.M., Plugge, C.M., De Vos, W.M., Smidt, H., et al., 2012.
767 Anaerobic benzene degradation under denitrifying conditions: Peptococcaceae as dominant
768 benzene degraders and evidence for a syntrophic process. Environ. Microbiol. 14, 1171-1181.
769 Van Hamme, J.D., Singh, A., Ward, O.P., 2003. Recent advances in petroleum microbiology.
770 Microbiol. Mol. Biol. Rev. 67, 503-549.
771 Wang, P., Li, X., Xiang, M., Zhai, Q., 2007a. Characterization of efficient aerobic denitrifiers isolated
772 from two different sequencing batch reactors by 16S rRNA analysis. J. Biosci. Bioeng. 103, 563-
773 567.
774 Wang, Q., Garrity, G.M., Tiedje, J.M., Cole, J.R., 2007b. Naive Bayesian classifier for rapid assignment
775 of rRNA sequences into the new bacterial taxonomy. Appl. Environ. Microbiol. 73, 5261-5267.

Wei T., 2013. Corrplot: visualization of a correlation matrix, Version 0.71. Compr R Arch Network, Vienna, Austria.

Wickham H., 2009. ggplot2: elegant graphics for data analysis. Springer Science and Business Media.

Wilson, L.P., Bouwer, E.J., 1997. Biodegradation of aromatic compounds under mixed oxygen/denitrifying conditions: a review. J. Ind. Microbiol. Biotechnol. 18, 116-130.

Yagi, J.M., Suflita, J.M., Gieg, L.M., DeRito, C.M., Jeon, C.O., Madsen, E.L., 2010. Subsurface cycling of nitrogen and anaerobic aromatic hydrocarbon biodegradation revealed by nucleic acid and metabolic biomarkers. Appl. Environ. Microbiol. 76, 3124–3134.

Yang, S., Wen, X., Zhao, L., Shi, Y., Jin, H., 2014. Crude oil treatment leads to shift of bacterial communities in soils from the deep active layer and upper permafrost along the China-Russia Crude Oil Pipeline route. PLoS ONE 9:e96552.

Yerushalmi, L., Lascourreges, J.F., Rhofir, C., Guiot, S.R., 2001. Detection of intermediate metabolites of benzene biodegradation under microaerophilic conditions. Biodegradation 12, 379–391.

Yuan K., Chen, B., Qing, Q., Zou, S., Wang, X., Luan, T., 2017. Polycyclic aromatic hydrocarbons (PAHs) enrich their degrading genera and genes in human-impacted aquatic environments. Environ. Pollut. 230, 936-944.

Zedelius, J., Rabus, R., Grundmann, O., Werner, I., Brodkorb, D., Schreiber, F., Ehrenreich, P., Behrends, A., Wilkes, H., Kube, M., Reinhardt, R., Widdel F., 2011. Alkane degradation under anoxic conditions by a nitrate-reducing bacterium with possible involvement of the electron acceptor in substrate activation. Environ. Microbiol. Rep. 3, 125–135.

Zhu, B., Bradford, L., Huang, S., Szalay, A., Leix, C., Weissbach, M., et al., 2017. Unexpected diversity and high abundance of putative nitric oxide dismutase (Nod) genes in contaminated aquifers and wastewater treatment systems. Appl. Environ. Microbiol. 83:e02750-16.

Zumft, W.G., 1997. Cell biology and molecular basis of denitrification. Microbiol. Mol. Biol. Rev. 61, 533-616.

ACCEPTED MANUSCRIPT

Figure Captions

Figure 1: **Total naphthalene and fluoranthene degradation.** Naphthalene (A,B) and fluoranthene (C, D) (μg) in L1 and L3, in sediments (brown color) and respective liquid medium (blue color) sampled during 0, 3, 6, 12, 30, and 63 weeks of incubation. Autoclaved controls (AC) after 63 weeks of incubation were also analyzed. The error bars represent standard deviation (n = 3). Different Greek letters (α, β, and δ) show the significant (ANOVA, $P < 0.05$) differences among PAHs measurements within each case.

Figure 2: **Heatmap of the percentile of the relative abundance.** The occurrence of taxa at the phylum level along the different treatments (un-spiked control (C), and spiked with naphthalene (N) and fluoranthene (F)) and different time series microcosms analyzed (week 12 and week 63) in L1 and L3 sediment samples arranged by hierarchical clustering.

Figure 3: **Heatmap for L1 sediments percentile of the relative abundance of PICRUSt predicted genes.** Genes involved in the nitrate dissimilatory reduction and aerobic and anaerobic PAH degradation metabolic pathways along the different treatments (un-spiked control (C), and spiked with naphthalene (N) and fluoranthene (F)) and different time series microcosms analyzed (week 12 and week 63) in L1 and L3 sediment samples.

Figure 4: Heatmap showing the significant Spearman correlations. Correlations between the specific genes related to the enzymes involved in the different nitrate reduction pathways and the genes involved in the metabolism of aerobic and anaerobic PAHs degradation pathways along L1 and L3 sediment samples.

ACCEPTED MANUSCRIPT

Figure 5: **Heatmap for L3 sediments percentile of the relative abundance of PICRUSt predicted genes**. Genes involved in the nitrate dissimilatory reduction and aerobic and anaerobic PAHs degradation metabolic pathways along the different treatments (un-spiked control (C), and spiked with naphthalene (N) and fluoranthene (F)) and different time series microcosms analyzed (week 12 and week 63) in L1 and L3 sediment samples.

ACCEPTED MANUSCRIPT

ACCEPTED MANUSCRIPT

Table 1: Water and organic matter (OM) contents (in percentage), and particle size fractions (in percentage of total dry weight), total viable counts, denitrification activity, hydrocarbon concentration (mean and standard deviation, n = 3) Different uppercase Greek letters (α and β) show the significant (*t*-test, $P < 0.05$) differences in parameters among L1 and L3 sediments.

Site	L1	L3
OM (%)	$1.7 \pm 0.2^{\alpha}$	$9.7 \pm 0.2^{\beta}$
H_2O (%)	$21 \pm 2^{\alpha}$	$48.7 \pm 0.6^{\beta}$
Grain size distribution (%)		
Silt and clay (<0.063 mm)	3.9	54.5
Fine sand (0.063–0.25 mm)	18.0	29.6
Medium sand (0.25–1 mm)	58.6	15.7
Very coarse sand (1–2 mm)	11.8	0.2
Gravel (>2 mm)	7.7	*n.d*
Total viable counts (CFU mL^{-1})		
NRM	$48337 \pm 22043^{\alpha}$	$53200 \pm 16462^{\alpha}$
BTB	$1433 \pm 281^{\alpha}$	$717 \pm 155^{\beta}$
Blue haloed colonies	$253 \pm 75^{\alpha}$	$23 \pm 15^{\beta}$
Denitrification potential (pmoles h^{-1} g^{-1})		
N_2O production potential rates	$4747 \pm 6679^{\alpha}$	$14778 \pm 1879^{\beta}$
N_2 production potential rates	$2138 \pm 5087^{\alpha}$	$20263 \pm 8363^{\beta}$
Hydrocarbon concentration (µg kg^{-1})		
Naphthalene	$19 \pm 2^{\alpha}$	$29 \pm 2^{\beta}$
Fluoranthene	$3.8 \pm 0.1^{\alpha}$	$97 \pm 3^{\beta}$
Total 16 EPA PAHs*	$53 \pm 3^{\alpha}$	$758 \pm 27^{\beta}$
Total petroleum hydrocarbons	$64000 \pm 3000^{\alpha}$	$260000 \pm 12000^{\beta}$

n.d stands for not detected;

NRM stands for nitrate reducing medium;

BTB stands for bromothymol blue medium

* Sum of the concentrations of the 16 PAHs considered priority by US EPA

Table 2: Concentration (µM) of NH_4^+, NO_2^-, NO_3^-, and production rates (pmol h^{-1} g^{-1}) of N_2O and N_2 in autoclaved Bushnell-Haas medium (BH), and in bottles with L1 sediments incubated as control (without PAHs), and spiked with naphthalene and fluoranthene at the beginning (0 weeks) and after 3, 6, 12, 30 and 63 weeks of incubation (mean ± standard deviation, n = 3). Autoclaved controls (after 63 weeks) were also included.

Treatments	NH_4^+ (*µM*)	NO_2^- (*µM*)	NO_3^- (*µM*)	N_2O (*pmol N_2O h^{-1} g^{-1}*)	N_2 (*pmol N_2 h^{-1} g^{-1}*)
BH	6537 ± 154	0 ± 0	6472 ± 23	0 ± 0	0
Control	6043 ± 247	23 ± 17	5977 ± 292	2124 ± 169	1093
Naphthalene	6000 ± 105	7 ± 3	6456 ± 180	2215 ± 408	0
Fluoranthene	6117 ± 225	10 ± 5	6387 ± 304	1357 ± 652	3297
3 weeks					
Control	6002 ± 120	165 ± 190	5043 ± 172	2949 ± 2484	0
Naphthalene	6133 ± 187	51 ± 15	5336 ± 544	1254 ± 1078	0
Fluoranthene	7022 ± 741	4 ± 5	5793 ± 64	1453 ± 940	0
6 weeks					
Control	6736 ± 377	1.0 ± 0.1	4335 ± 123	115 ± 115	61
Naphthalene	6727 ± 290	4.2 ± 0.1	4775 ± 116	52 ± 52	442
Fluoranthene	6807 ± 154	0.3 ± 0.5	4417 ± 217	935 ± 749	4305
12 weeks					
Control	7199 ± 420	10 ± 18	5796 ± 372	3618 ± 3323	0
Naphthalene	6858 ± 392	28 ± 24	6612 ± 147	2282 ± 274	239
Fluoranthene	7332 ± 1182	0.27 ± 0.04	6331 ± 727	161 ± 161	102
30 weeks					
Control	7064 ± 311	2 ± 2	5111 ± 275	635 ± 72	0
Naphthalene	6992 ± 105	17 ± 8	5247 ± 23	186 ± 8	883
Fluoranthene	6384 ± 289	1 ± 2	4804 ± 303	7864 ± 5947	0
63 weeks					
Control	7102 ± 626	5 ± 6	4819 ± 236	2768 ± 2768	0
Naphthalene	6949 ± 157	123 ± 173	5088 ± 77	9677 ± 6866	0
Fluoranthene	6767 ± 145	31 ± 1	3737 ± 398	6058 ± 4147	0
Autoclaved (63 weeks)					
Naphthalene	7240 ± 572	0.5 ± 0.3	5704 ± 442	40 ± 40	0
Fluoranthene	7588 ± 915	71 ± 77	5399 ± 432	0 ± 0	517

ACCEPTED MANUSCRIPT

Table 3: Concentration (µM) of NH_4^+, NO_2^-, NO_3^-, and production rates (pmol h^{-1} g^{-1}) N_2O and N_2 in autoclaved Bushnell-Haas medium (BH), and in bottles with L3 sediments incubated as control (without PAHs), and spiked with naphthalene and fluoranthene at the beginning (0 weeks) and after 3, 6, 12, 30 and 63 weeks of incubation (mean ± standard deviation, n = 3). Autoclaved controls (after 63 weeks) were also included. Autoclaved potassium nitrate (KNO3) was added at week 33 and also at week 60, since between weeks 33 and 60 all the nitrate get reduced in all bottles, including controls.

Treatments	NH_4^+ (*µM*)	NO_2^- (*µM*)	NO_3^- (*µM*)	N_2O (*pmol N_2O h^{-1} g^{-1}*)	N_2 (*pmol N_2 $h^{-1}g^{-1}$*)
BH	6537 ± 154	0 ± 0	6472 ± 23	0 ± 0	0
Control	4979 ± 330	8 ± 5	4152 ± 74	1418 ± 907	18622
Naphthalene	5146 ± 336	6 ± 4	3872 ± 111	18161 ± 6717	1753
Fluoranthene	4854 ± 131	7 ± 3	4005 ± 116	18050 ± 4444	11753
3 weeks					
Control	5481 ± 411	2 ± 1	2311 ± 148	46706 ± 2844	0
Naphthalene	5168 ± 124	9 ± 8	1975 ± 15	39518 ± 9047	0
Fluoranthene	4999 ± 853	1.6 ± 0.2	2009 ± 394	23518 ± 17823	3532
6 weeks					
Control	5012 ± 223	0.41 ± 0.02	1438 ± 68	0 ± 0	82197
Naphthalene	4722 ± 387	0.66 ± 0.07	1843 ± 1163	67433 ± 23433	36220
Fluoranthene	5064 ± 570	0.12 ± 0.04	953 ± 214	73268 ± 14175	25469
12 weeks					
Control	4651 ± 269	1.0 ± 0.2	42 ± 15	72463 ± 5417	0
Naphthalene	5862 ± 276	22 ± 21	654 ± 756	71399 ± 18072	47854
Fluoranthene	6028 ± 345	2 ± 3	240 ± 346	8347 ± 3750	84362
30 weeks					
Control	5494 ± 48	0.5 ± 0.1	4 ± 2	249 ± 140	34
Naphthalene	5502 ± 214	0.52 ± 0.02	5 ± 2	99 ± 9	19
Fluoranthene	5599 ± 214	0.6 ± 0.1	3 ± 1	95 ± 2	30
63 weeks					
Control	7461 ± 87	4 ± 1	5828 ± 303	69139 ± 6677	68567
Naphthalene	7617 ± 131	10 ± 4	5749 ± 13	87004 ± 60178	51076
Fluoranthene	8016 ± 73	2 ± 1	5651 ± 215	109345 ± 0	8041
Autoclaved (63 weeks)					
Naphthalene	6098 ± 840	5 ± 6	3630 ± 84	13151 ± 12910	0
Fluoranthene	6641 ± 832	2 ± 2	3654 ± 482	268 ± 268	0

ACCEPTED MANUSCRIPT

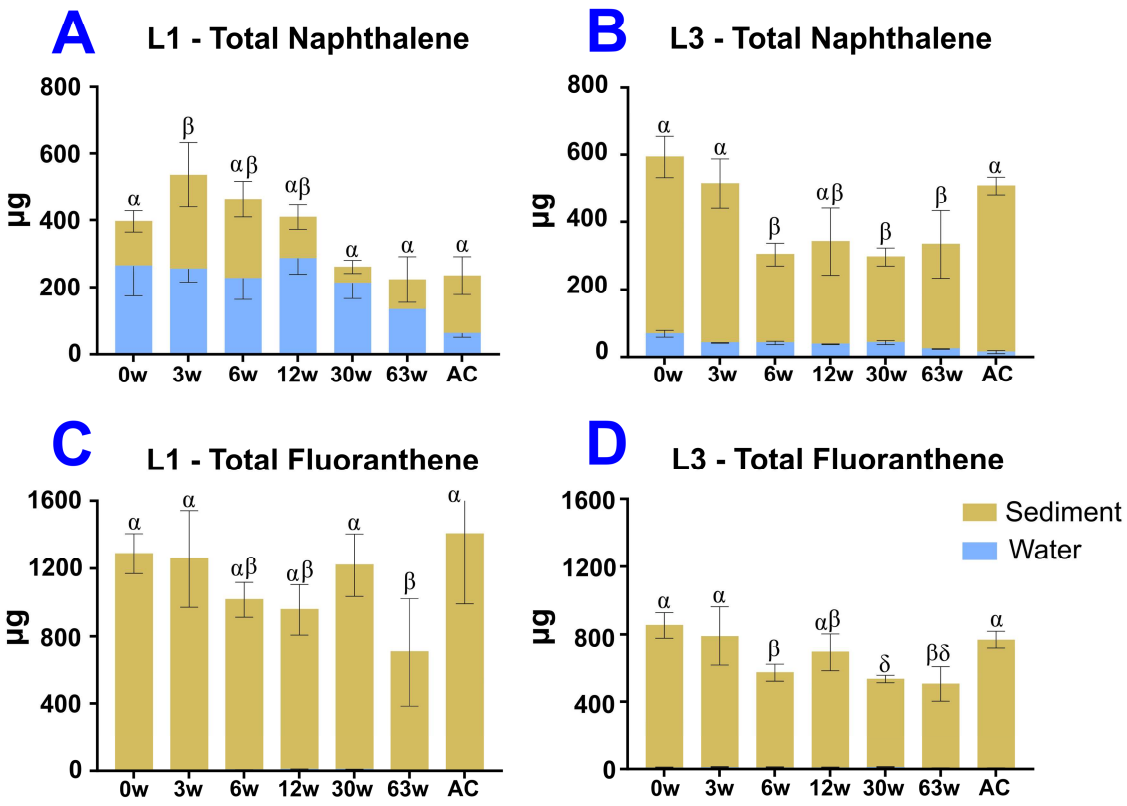

ACCEPTED MANUSCRIPT

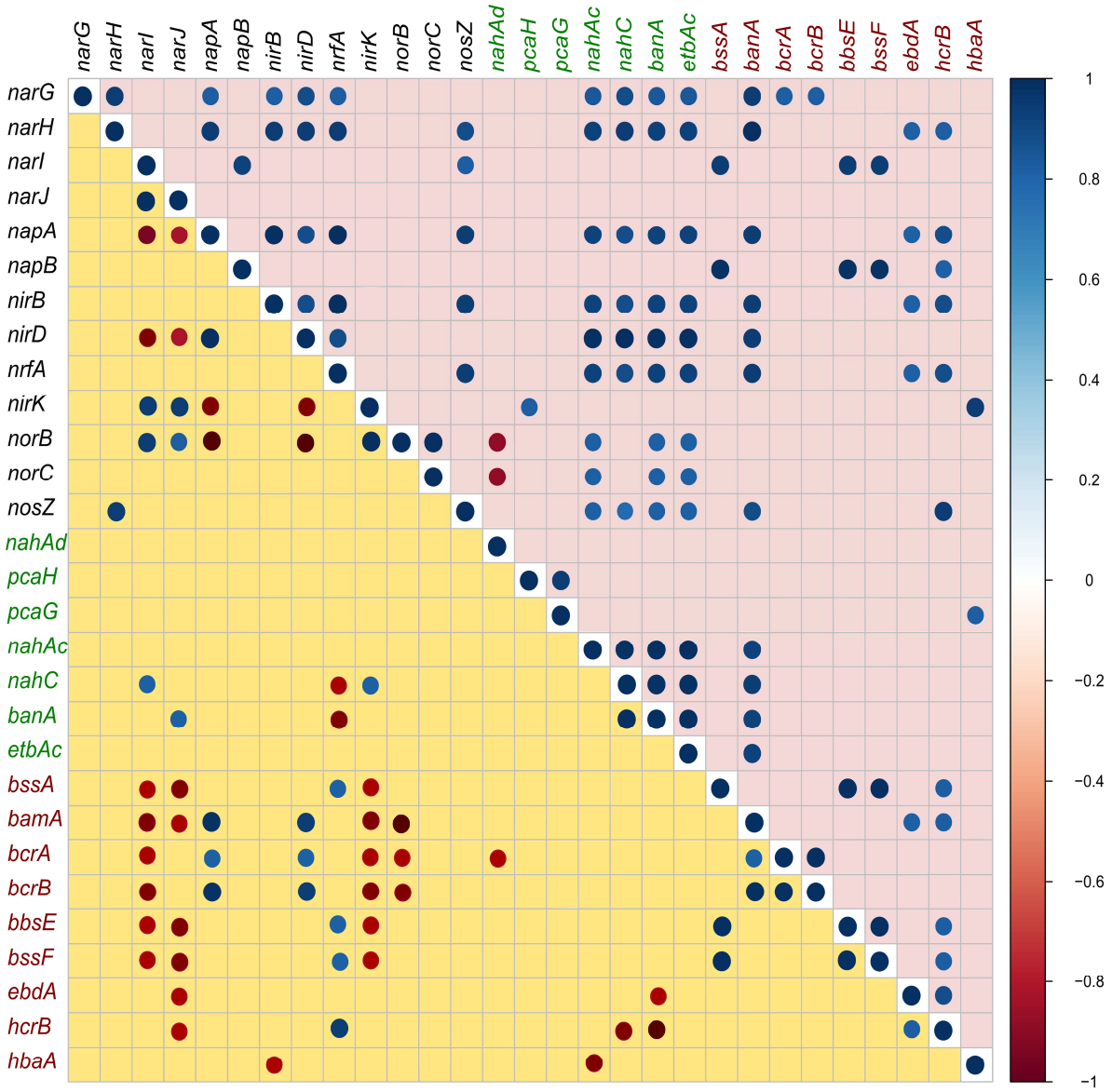

Genes involved in aerobic PAHs degradation pathways

Genes involved in anaerobic PAHs degradation pathways

Genes involved in dissimilatory reduction of nitrate pathways

L1 sediments

L3 sediments

ACCEPTED MANUSCRIPT

Highlights

- Degradation dynamics of naphthalene and fluoranthene varied with sediment type.
- Microbial community structure was influenced by sediment type and incubation time.
- Experiment induced higher effect in prokaryotic communities of sandy sediments.
- Shifts in PAHs degradation and nitrate-reducing pathways predicted genes.
- Dissimilatory nitrate-reducing pathways involvement in PAH degradation.

ACCEPTED MANUSCRIPT